JOC Article

Self-Assembly, Binding, and Dynamic Properties of Heterodimeric Porphyrin Macrocycles

Pablo Ballester,*,† Antoni Costa,‡ Pere M. Deyà,‡ Antonio Frontera,‡ Rosa M. Gomila,‡ Ana I. Oliva,|| Jeremy K. M. Sanders,§ and Christopher A. Hunter*,¶

ICREA and Institute of Chemical Research of Catalonia (ICIQ), 43007-Tarragona, Spain, Departament de Química, Universitat de les Illes Balears, 07122-Palma de Mallorca, Spain, University Chemical Laboratories, Lensfield Road, Cambridge CB2 1EW, United Kingdom, and Centre for Chemical Biology, Krebs Institute for Biomolecular Science, Department of Chemistry, University of Sheffield, Sheffield S3 7HF, United Kingdom

pballester@iciq.es; c.hunter@sheffield.ac.uk

Received March 16, 2005

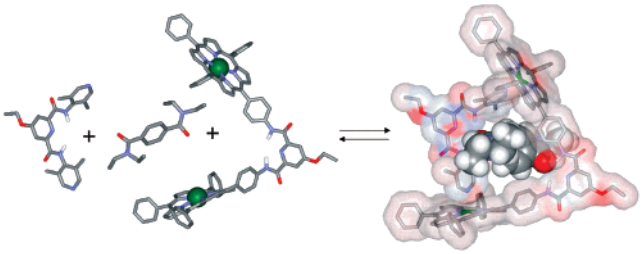

A series of heterodimeric tetralactam macrocycles have been self-assembled using two kinetically labile zinc porphyrin-pyridine interactions. The stability constants have been determined by UV−vis titrations in $CHCl_3$. The stability constants depend on the degree of preorganization of the linker units connecting the interacting groups. The ability of the self-assembled macrocycles to bind a terephthalamide guest was also investigated. One of the macrocycles was used for the construction of a [2]rotaxane. The dynamic properties of this system provide insight into the exchange mechanisms that operate in complex noncovalent assemblies.

Introduction

Interlocked molecular complexes are appealing systems for the construction of simple molecular-level machines.[1] From this viewpoint, [2]pseudorotaxane and [2]rotaxane systems comprising a macrocycle (wheel) threaded by a linear molecule (axle) constitute a very attractive and interesting proposition. In most cases, the construction of these molecular architectures employs a two-molecule approach (macrocycle and linear component), both linked by covalent bonds.[2] Recently, Jeong[3] and one of us[4] reported different examples of noncovalent assembly of [2]pseudorotaxanes and [2]rotaxanes using a three-molecule approach. In both cases, a tetralactam macrocycle was self-assembled using reversible coordinate bonds and was employed as the wheel component of the interlocked molecular system. Herein, we report our continued efforts to devise rotaxane-like structures, that because of the kinetic lability of the zinc-pyridine interaction can reversibly assemble from and dissociate into their components under thermodynamic conditions. A series of dinuclear macrocycles **1** (Figure 1) were designed as the wheel component. The symmetry of the two complementary components of **1** simplifies their synthesis compared to the porphyrin dimer **2** (Figure 1) previously reported.[4] The fact that metallomacrocycle **1** is not assembled through a self-coordination process implies that its formation can be achieved in the presence of a slight excess of bisporphyrin **4** with respect to bispyridyl **3** (Scheme 1) or vice versa. Under these conditions when a suitable guest is added, it should be possible to study

† ICREA and ICIQ. Phone: +34 977 920 206; fax: +34 977 920 221.
‡ Universitat de les Illes Balears.
§ University Chemical Laboratories.
|| ICIQ.
¶ University of Sheffield.

(1) (a) Sauvage, J.-P. *Molecular Machines and Motors*; Springer-Verlag: Berlin, 2001; Vol. 99. (b) Balzani, V.; Credi, A.; Raymo, F. M.; Stoddart, J. F. *Angew. Chem., Int. Ed.* **2000**, *39*, 3348−3391.

(2) (a) Schalley, C. A.; Beizai, K.; Vögtle, F. *Acc. Chem. Res.* **2001**, *34*, 465−476. (b) Bottari, G.; Leigh, D. A.; Perez, E. M. *J. Am. Chem. Soc.* **2003**, *125*, 13360−13361 and references therein.

(3) Jeong, K.-S.; Choi, J. S.; Chang, S.-Y.; Chang, H.-Y. *Angew. Chem., Int. Ed.* **2000**, *39*, 1692−1695.

(4) Hunter, C. A.; Low, C. M. R.; Packer, M. J.; Spey, S. E.; Vinter, J. G.; Vysotsky, M. O.; Zonta, C. *Angew. Chem., Int. Ed.* **2001**, *40*, 2678−2682.

10.1021/jo0505369 CCC: $30.25
Published on Web 07/27/2005

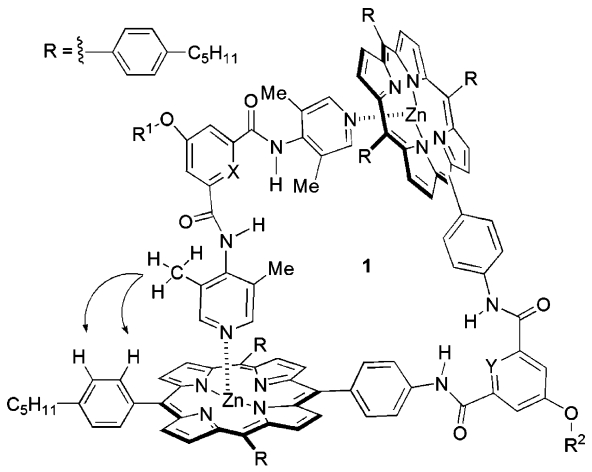

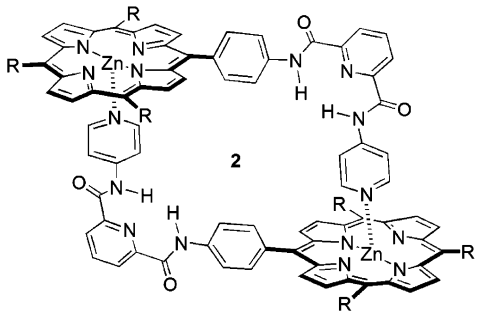

FIGURE 1. Structural formulas of the self-assembled macrocycles. The arrows show intermolecular NOEs observed in a ROESY experiment for **1aa**. See text for details.

simultaneously the exchange dynamics of opening the macrocycle and host−guest binding. The heteromeric composition of **1** also allows us to assess the effects of preorganization of the 2,6-dicarboxamidopyridine linker versus the analogous 2,6-dicarboxamidobenzene for each component in the self-assembly of the macrocycle.

The 2,6-dicarboxamidopyridine unit has internal hydrogen bonds and is expected to adopt a conformation that orients its two arms approximately perpendicular to one another.[5] The self-assembly of rectangular macrocycles using a self-complementary porphyrin-pyridine unit as in **2** (self-coordination) or complementary bispyridine and bisporphyrin units as in **1** is favored when the corner angles are close to 90°. In our design, two of the corners are provided by the conformation adopted by the 2,6-dicarboxamidopyridine (or benzene) units and the other two by the axial interaction of the pyridine ligand with the zinc porphyrin.

Results and Discussion

The synthesis of the bispyridyl ligands **3** and zinc bisporphyrins **4** is outlined in Scheme 1. The dichlorides

SCHEME 1. Synthesis of the Bispyridyl Ligands 3 and Zinc Bisporphyrins 4[a]

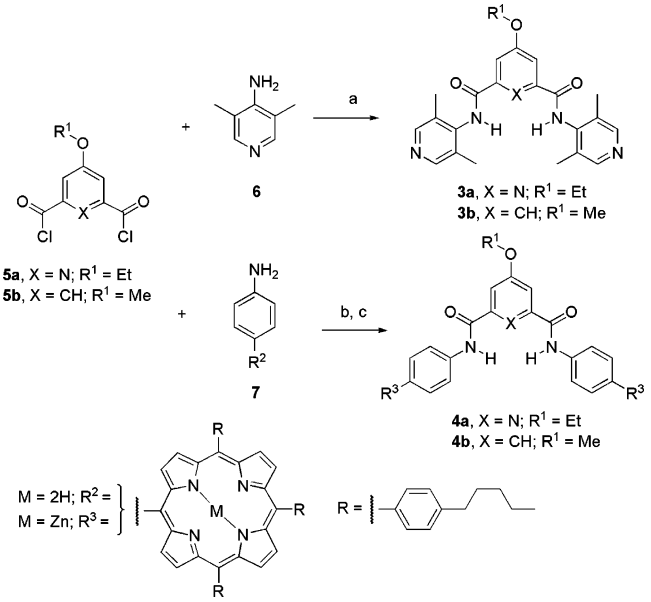

[a] Reagents and conditions: (a) *i*-Pr_2NEt, CH_2Cl_2, 0 °C to reflux. (b) Et_3N, CH_2Cl_2, 0 °C to reflux. (c) $Zn(OAc)_2/CH_2Cl_2$:CH_3OH (3:1).

5a[6] and **5b**,[7] 4-amino-3,5-lutidine **6**,[8] and the aminoporphyrin **7**[9] were prepared according to literature procedures. Reaction of 2.2 equivalents of **6** with the diacid chlorides **5a**−**b** in dry methylene chloride and in excess Hünig's base afforded, after trituration with diethyl ether, ligands **3a**−**b** in 80 and 22% yield, respectively. Coupling the diacid chlorides **5a**−**b** with aminoporphyrin **7** was accomplished by dropwise addition of a methylene chloride solution of the chloride into a solution of the same solvent, previously cooled at 0 °C containing 2 equivalents of the aminoporphyrin and excess triethylamine. Column chromatography of the crude products allowed the isolation of the free base bisporphyrins in 46 and 42% yield, respectively. Metalation was accomplished almost quantitatively using a solution of zinc acetate in CH_2Cl_2:CH_3OH (3:1) affording the zinc bisporphyrins **4a**−**b**.

The self-assembly of **1** was studied at 295 K in chloroform using ^1H NMR and UV−vis absorption spectroscopy. A chloroform solution of the bisporphyrin component **4** maintained at constant concentration was titrated by adding incremental amounts of the bispyridyl component **3**. The maximum in the UV−vis absorption spectra for the Soret band of the free zinc bisporphyrins **4** is centered at 420 nm. On addition of bispyridyl ligands **3**, a new Soret band appeared at 430 nm with an isosbestic point in all cases. This 10-nm red shift is characteristic of coordination of a pyridine ligand to a zinc porphyrin. Analysis of the UV−vis binding curves

(5) Hunter, C. A.; Sarson, L. D. *Angew. Chem., Int. Ed. Engl.* **1994**, *33*, 2313−2316.

(6) Markees, D. G.; Kidder, G. W. *J. Am. Chem. Soc.* **1956**, *78*, 4130−4135.

(7) (a) Lee, S. B.; Hong, J.-I. *Tetrahedron Lett.* **1998**, *39*, 4317−4320. (b) Fosdick, L. S.; Fancher, O. E. *J. Am. Chem. Soc.* **1941**, *63*, 1277−1279. (c) Calandra, J. C.; Svarz, J. J. *J. Am. Chem. Soc.* **1950**, *72*, 1027−1028.

(8) Essery, J. M.; Schofield, K. *J. Chem. Soc.* **1960**, 4953−4959.

(9) Gardner, M.; Guerin, A. J.; Hunter, C. A.; Michelsen, U.; Rotger, C. *New J. Chem.* **1999**, *23*, 309−316.

TABLE 1. Stability Constants (M^{-1}) and Effective Molarities (*EM*) Measured at 295 K for the Self-Assembled Macrocycles 1 Determined by UV−Vis Titrations

macrocycle	$K_{stability}$ (M^{-1})	*EM* (M)[c]
2	2×10^8 [a]	6
3a + **4a** ⇔ **1aa**	$(1.3 \pm 0.2) \times 10^7$ [b]	3
3b + **4a** ⇔ **1ba**	$(8.7 \pm 0.8) \times 10^6$ [b]	1
3a + **4b** ⇔ **1ab**	$(1.1 \pm 0.6) \times 10^5$ [b]	0.02
3b + **4b** ⇔ **1bb**	$(2.9 \pm 0.4) \times 10^5$ [b]	0.04

[a] Value taken from ref 5 and determined in CH_2Cl_2 solution. [b] Determined in $CHCl_3$ solution. [c] $EM = K_{stability}/K_m^2$. Calculated using the K_m value determined in the corresponding solvent.

showed that a simple 1:1 complex was formed and from fitting the data to the theoretical binding isotherm, the stability constants were determined.[10] Effective molarities (*EM*) or chelation factors are useful for quantifying cooperativity in intramolecular interactions and host−guest complementarity in divalent binding. The *EM* for these systems can be quantified using the following relationship $K_{stability} = K_m^2\ EM$.[11] A value of $K_m = 5.6 \times 10^3\ M^{-1}$ (intrinsic binding constant for the zinc-pyridine interaction) was determined previously for a reference complex of a monomeric zinc porphyrin with a similar monopyridine ligand in methylene chloride.[5] We determined that the association constants for the same reference complex in chloroform is $K_m = 2.2 \times 10^3\ M^{-1}$.

The stability constants and *EM* values for each complex are summarized in Table 1. To take solvent effects into account, the *EM* values are calculated using the binding constant of the reference complex (K_m) measured in the same solvent where the titration was performed. Thus, the relative stabilities of the macrocycles are based on the reported *EM* values. When these titrations were repeated at a concentration of 10^{-3} M using ^{1}H NMR spectroscopy, the signals due to the α-pyridine proton ($\Delta\delta = -6.2$ ppm) and the pyridine methyl group ($\Delta\delta = -1.3$ ppm) were highly upfield shifted on complexation, indicating that the pyridine sits over the face of the porphyrin ring. Analogous upfield shifts were also observed for these protons when the other three complexes **1ab, 1ba**, and **1bb** were formed. A ROESY experiment on **1aa** revealed intermolecular contacts between the pyridine methyl protons and the aromatic protons of the meso-phenyl substituents on the porphyrin ring (see Figure 1). This result is consistent with the macrocyclic structure proposed for **1aa**.

The data in Table 1 indicate that all macrocycles **1** are assembled quantitatively at mM concentrations. In all cases, the complementarity between the bispyridine and bisporphyrin units, quantified by the *EM* value, is inferior to that observed between the two aminoporphyrin units that self-coordinate in macrocycle **2**. When the 2,6-dicarboxamidopyridine linker is present in the bisporphyrin component (**4a**), the most stable macrocycle is obtained. However, the nature of the linker in the bispyridyl component has little or no effect on the stability of the macrocycle. Simple molecular modeling

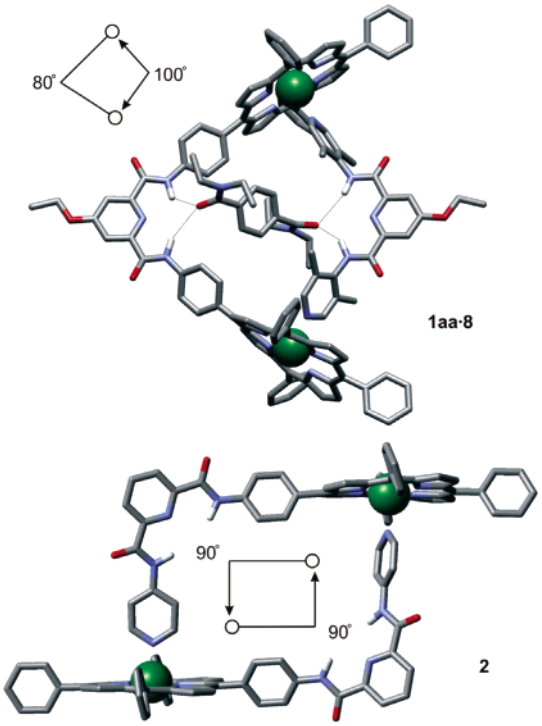

FIGURE 2. Minimized structures (MMFF94 force field) of **1aa•8** and **2** showing the different geometries of the dimer. Nonpolar hydrogen atoms and pentyl substituents have been omitted for clarity.

studies[12] show that the formation of macrocycle **1** requires that the zinc bisporphyrin component has a syn arrangement of the amides. This conformation is favored in the 2,6-carboxamidopyridine linker, placing the two porphyrin rings in an almost perpendicular orientation. This linker has internal hydrogen bonds which reduces the 120° angle expected for meta-substituted arenes to approximately 96° (Figure 2).[5,12]

In contrast, the bispyridyl component can span the gap between the two porphyrins equally well regardless of the nature of the linker.[13] The most likely explanation for the difference between the *EM* values of **2** and **1aa** is due to a geometric mismatch in the heteromeric system. Macrocycle **2** forms a rectangular structure with four right-angled corners and two sets of parallel sides of equal length. The X-ray crystal structure shows that **2** is essentially strain-free.[4] In **1aa**, the parallel sides are not of equal length, and the energy-minimized structure of **1aa** reveals a quadrilateral geometry that requires distortion of the 2,6-dicarboxamidopyridine linkers away from the ideal 90° geometry. If right angles are maintained for the two zinc-pyridine interactions, the bisporphyrin unit needs to reduce the 2,6-dicarboxamidopyridine angle and the bispyridyl component needs to open

(10) SPECFIT, ver 3.0, from Spectra Software Associates. Gampp, H.; Maeder, M.; Meyer, C. J.; Zuberbühler, A. D. *Talanta* **1985**, *32*, 95−101.

(11) Anderson, H. L.; Anderson, S.; Sanders, J. K. M. *J. Chem. Soc., Perkin Trans. 1* **1995**, 2231−2245.

(12) The MMFF94 was used as implemented in Macromodel 6.0, except that the charges on the Zn atoms and N atoms coordinated to it were modified. Mohamadi, F.; Richards, N. G. J.; Guida, W. C.; Liskamp, R.; Lipton, M.; Caulfield, C.; Chang, G.; Hendrickson, T.; Still, W. C. *J. Comput. Chem.* **1990**, *11*, 440.

(13) Differences in the conformation adopted by the bisporphyrins **4a** and **4b** may cause changes in the geometry of the zinc porphyrin-pyridine interaction contributing also to the observed difference in stability. Gomila, R. M.; Quiñonero, D.; Rotger, C.; Garau, C.; Frontera, A.; Ballester, P.; Costa, A.; Deyà, P. M. *Org. Lett.* **2002**, *4*, 399−401.

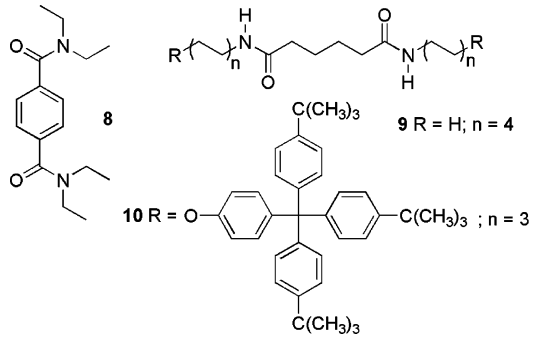

FIGURE 3. Structures of the amides used in the titrations and the VT NMR experiments.

TABLE 2. Association Constants (K_a ± 20%) Determined by ^{1}H NMR Titrations in $CDCl_3$ of Macrocycles 1 with Diamide 8 at 298 K

macrocycle	1aa	1ab	1ba	1bb
K_a (M^{-1})	160	550	260	320

this angle slightly to achieve a ditopic interaction (Figure 2).[14]

Next, we set out to investigate the binding properties of macrocycles **1** using ^{1}H NMR titration with *N,N,N′,N′*-tetraethyl terephthalamide **8** (Figure 3). This compound can form up to four hydrogen bonds with the amide groups directed into the cavity of **1** and has been used previously as a guest with similar tetralactam receptors.[3,4,15] For the titration of **1aa**, the NH signals of the bisporphyrin and bispyridine components (see Figure S4) shifted downfield 0.16 and 0.44 ppm, respectively, upon addition of 4.6 equiv of **8**, indicative of the formation of hydrogen bonds between the amide NHs of **1aa** and the carbonyl oxygens of **8**. For **1ba**, the same amount of **8** caused a downfield shift of the NHs of the bisporphyrin and bispyridine components of 0.14 and 0.28 ppm, respectively. In the case of **1ab**, it was only possible to follow and measure the downfield shift of the NHs of the bispyridine component which was 0.27 ppm when 4.6 equiv of **8** are added. The NH signal of the bisporphyrin unit of **1ab** was too broad to be used for the titration experiment. For **1bb**, both types of NH signals were either too broad or overlapped with other proton signals in the aromatic region. In this case, we followed the downfield shift experienced by the proton signal assigned to the methyl ether of the bisporphyrin component upon addition of **8** (0.19 ppm when 4.6 equiv of **8** are added). The titration data obtained for the chemical shift change of the above-mentioned signals were fitted to a 1:1 binding model, and the calculated association constants are shown in Table 2. When more than one signal was used to calculate the association constant, the value reported is an average value.

The binding affinities are all of the same order of magnitude and are comparable to those reported previously for covalent tetralactam macrocycles.[16] The substitution of the 2,6-carboxamidopyridine linker with a closely related benzene linker has a relatively small effect on the binding constants. The signal due to the aromatic protons of **8** shows an upfield complexation induced change in chemical shift in all of the complexes (estimated $\Delta\delta_{max} = -1.0$ to -1.5 ppm) which suggests that the mode of binding involves the formation of a threaded H-bonded complex (Figure 2).[17]

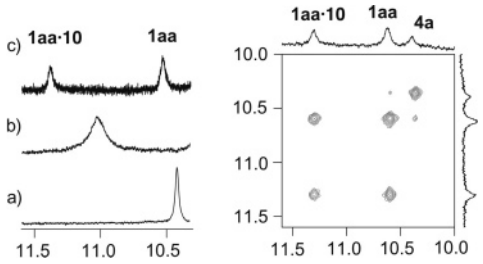

FIGURE 4. Left: downfield regions of ^{1}H NMR spectra in $CDCl_3$ at 253 K (a) [**1aa**] = 1 mM; (b) [**1aa**] = 1 mM and [**9**] = 4 mM; (c) [**1aa**] = 1 mM and [**10**] = 4 mM. Right: Expansion of the EXSY experiment at 253 K; [**1aa**] = 1 mM, $[\mathbf{4a}]_{free}$ = 0.2 mM, and [**10**] = 4 mM.

Other evidence for the formation of pseudorotaxane and rotaxane structures with these macrocycles came from dynamic ^{1}H NMR studies carried out with diamides **9** and **10**. While macrocycle **1aa** forms complexes with similar structure and stability with **9** and **10** (K_a = 184 and 160 M^{-1}, respectively), their dynamic properties are quite different.

On cooling a 1 mM chloroform solution of **1aa** containing 4 equivalents of diamide **10** to 253 K, the signal due to the amides of the bisporphyrin component (**4a**) split into two signals. The rest of the signals of **1aa** become broad upon cooling and no other splitting of signals could be clearly observed. One signal had a chemical shift very close to that of pure **1aa**,[18] and the other was downfield shifted, indicative of hydrogen bonding. We conclude that the splitting is due to slow exchange between free and bound **1aa**. Under identical conditions with a mixture of **1aa** and **9**, no splitting was observed for the same signal. In this case, only broadening of the signal was observed, and the chemical shift was intermediate between that of the free and bound signals of **1aa** (Figure 4). This is due to fast exchange between the free and bound species in this case. Although the two complexes, **1aa•9** and **1aa•10**, have similar structures and thermodynamic stabilities, they clearly have quite different dynamic properties. The most likely explanation is that complex **1aa·9** has a pseudorotaxane structure, while **1aa·10** is a rotaxane. Thus, while the exit or entry of **9** into the cavity of **1aa** does not require disruption of the macrocycle, the rate-determining step for exchange of **10** involves opening the macrocycle by breaking zinc-pyridine interactions, because the bulky stopper groups do not fit into the cavity (Figure 5).

(14) Bisporhyrin **4a** is a flexible molecule, for example, about the porphyrin meso bond and so a range of strained conformations are possible for macrocycle **1aa**. The structure depicted in Figure 2 is only an energy minimum.

(15) Chang, S.-Y.; Um, M.-C.; Uh, H.; Jang, H.-Y.; Jeong, K.-S. *Chem. Commun.* **2003**, 2026−2027.

(16) Chang, S.-Y.; Kim, H. S.; Chang, K.-J.; Jeong, K.-S. *Org. Lett.* **2004**, *6*, 181−184.

(17) Intermolecular NOEs observed in a ROESY experiment on **1aa·8** are also in agreement with a threading binding mode.

(18) The small chemical shift difference between the bisporphyrin amide signals of pure **1aa** compared with free **1aa** in the presence of **10** is probably due to some aggregation at low temperatures.

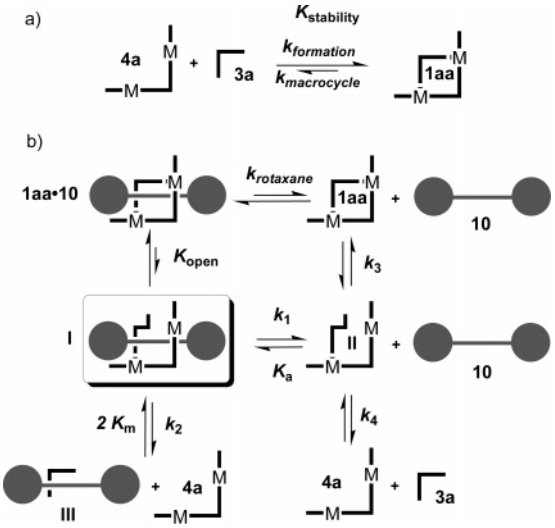

FIGURE 5. Processes involved in the exchange of macrocycle **1aa** and its components (a) and rotaxane **1aa·10**, macrocycle **1aa**, and free bisporphyrin **4a** (b). The key intermediate **I** is highlighted.

The rotaxane exchange mechanism can be probed by comparing the rate of exchange of free **1aa** with the rotaxane **1aa·10** and the rate of exchange of free **4a** with the macrocycle **1aa**.[19] Both exchange processes are slow on the NMR time scale at 253 K, and the rate constants were therefore determined simultaneously using two-dimensional exchange spectroscopy (2D-EXSY).[20] The rate constants were determined using the diagonal and cross-peak areas for the NH signals of **1aa** (free and bound) and the free bisporphyrin **4a**.[21] The rate constant $k_{rotaxane}$ for the interconversion of **1aa·10** and free **1aa** is 13 (±1) s^{-1}, corresponding to an activation energy ($\Delta G^{\ddagger}$) of 13.4 kcal mol^{-1}. The rate constant $k_{macrocycle}$ for exchange between the bisporphyrin in the macrocycle **1aa** and free bisporphyrin **4a** is 2.2 (±0.3) s^{-1}, giving an activation energy ($\Delta G^{\ddagger}$) of 14.4 kcal mol^{-1}. No cross-peaks were observed between the amide of the rotaxane **1aa·10** and the free bisporphyrin **4a**. Consequently, at this temperature, interconversion between the rotaxane **1aa·10** and its components macrocycle **1aa** and diamide **10** is faster than any of the possible exchanges involving the free bisporphyrin **4a**. Why is this type of dynamic behavior observed in this system?

The exchange of the macrocycle **1aa** with its component parts, **3a** and **4a,** can be considered as a straightforward dissociation process breaking two zinc-pyridine interactions (Figure 5a). For this dissociation, the first-order rate constant for fully breaking the macrocycle ($k_{macrocycle}$) was determined using the EXSY experiment as $k_{macrocycle}$ = 2.2 (±0.3) s^{-1} (T = 253 K). Using the macrocycle stability constant (1.3×10^7 M^{-1}, T = 295 K, Table 1) and assuming that it is not sensitive to small temperature changes, the second-order rate constant for macrocycle formation can be estimated $k_{formation} \approx 2.9 \times 10^7$ M^{-1} s^{-1} ($K_{stability} = k_{formation}/k_{macrocycle}$). This implies that the formation of the highly stable macrocycle **1aa** is close to diffusion controlled, as expected for a system where there are no significant kinetic barriers. The binding sites of **3a** and **4a** are sterically accessible, and desolvation during complexation requires only a small activation energy.

Figure 5b illustrates the processes that are important in the case of the exchange of rotaxane **1aa·10** and its components. Here, the key intermediate is **I** where only one of the zinc-pyridine interactions is broken. This species can close again to regenerate the rotaxane **1aa•10**, and this process must be very rapid setting up an equilibrium between the rotaxane and **I**. We can estimate the equilibrium constant K_{open} from the *EM* for cyclization of **1aa** (*EM* = 3 M, T = 295 K, Table 1) and the binding constant of the reference complex ($K_m = 2.2 \times 10^3$ M^{-1}). Thus, $K_{open} = 2/EM\ K_m = 3 \times 10^{-4}$. The factor of 2 accounts for the probability of opening one of two zinc-pyridine interactions. Intermediate **I** could subsequently lose either the guest **10** with rate constant k_1 or break the second zinc-pyridine interaction to lose the bisporphyrin **4a** with rate constant k_2. The rate constants, k_1 and k_2, for these processes are determined by the strengths of the interactions to be broken. Thus, if we assume a diffusion-controlled rate for the formation process of intermediate **I** from its components **II** and **10** or **III** and **4a** (from above, $k_{formation} = 2.9 \times 10^7$ M^{-1} s^{-1}) and estimate association constants for each process on the basis of the interactions involved (K_a = 160 M^{-1} for the formation of **I** from **II** and **10**, see Table 2, and $2K_m = 5 \times 10^3$ M^{-1} for the formation of **I** from **III** and **10**), we can estimate the first-order rate constants for the two competitive processes as $k_1 = k_{formation}/K_a = 18 \times 10^4$ s^{-1}, and $k_2 = k_{formation}/2K_m = 5.8 \times 10^3$ s^{-1} (the statistical factor of 2 relates to the asymmetry of **I**). The rate of loss of **4a** from **I** is an order of magnitude smaller than the rate constant of loss of **10**, because the strengths of the interactions holding the different units in place are very different. The partially open macrocycle (**II**) formed by the loss of **10** can now either lose **4a** (k_4 in Figure 5b) or close to regenerate **1aa** (k_3 in Figure 5b). No interactions must be broken in the latter process, so $k_3 \gg k_4$. This dynamic scheme explains why there is no direct exchange of **4a** with the rotaxane **1aa•10** in the EXSY spectrum in Figure 4. The analysis above allows us to estimate the expected rate constant for the exchange of the rotaxane with the macrocycle, $k_{rotaxane} = K_{open}\ k_1$ = 54 s^{-1}. This value is higher than the observed value of 13 s^{-1}, indicating that there is an additional 0.7 kcal mol^{-1} strain energy in the transition state for escape of **10**.

Conclusion

In conclusion, we have demonstrated the quantitative self-assembly of a series of heterodimeric tetralactam macrocycles at mM concentrations in $CDCl_3$ using two kinetically labile zinc porphyrin-pyridine interactions. We have studied the effect of preorganization of the linker on the stability of the macrocycles. The macrocycles feature a cavity with inwardly directed hydrogen bond donors that make them molecular hosts for terephthala-

(19) It has been proposed for similar systems that the exchange between the components of the rotaxane occurs by breaking just one coordinative bond (see refs 3 and 4), but no determination of the rate constant for the exchange of the subunits of the self-assembled macrocycle has been carried out.

(20) Pons, M.; Millet, O. *Prog. Nucl. Magn. Reson. Spectrosc.* **2001**, *38*, 267−324. Perrin, C. L.; Dwyer, T. J. *Chem. Rev.* **1990**, *90* (6), 935−67.

(21) D2DNMR (PC version). Abel, E. W.; Coston, T. P. J.; Orrell, K. G.; Sik, V.; Stephenson, D. *J. Magn. Reson.* **1986**, *70* (1), 34−53.

mide and adipamide guests. We have used one of the self-assembled macrocycles for the construction of a [2]-rotaxane. The dissociation rate for the interconversion between the components of the [2]rotaxane (macrocycle and linear bisamide) is faster than complete dissociation of the macrocycle in both the free and bound states.

Experimental Section

Titrations and Data Analysis. ^{1}H NMR and UV−vis titrations were performed by adding solutions of the guest (**8**, **9**, **10** for the ^{1}H NMR titrations or **3a**−**b** for the UV−vis titrations) to a solution of the host (macrocyle **1** for the ^{1}H NMR titrations or zinc bisporphyrin **4a**−**b** for the UV−vis titrations) in either a 5-mm NMR tube or a 1-cm path cuvette using microliter syringes. In both types of titration experiments, the host was present in the guest solution at the same concentration as that in the NMR tube or cuvette to avoid dilution effects. Deacidified chloroform and deacidified deuterochloroform were used as solvents for the UV−vis and ^{1}H NMR titrations, respectively. UV−vis spectrophotometric titrations were analyzed by fitting the whole series of spectra at 1-nm intervals using the software SPECFIT 3.0 from Spectrum Software Associates, PMB 361, 197M Boston Post Road West, Marlborough, MA 01752 (e-mail: SpecSoft@compuserve.com), which uses a global system with expanded factor analysis and Marquardt least-squares minimization to obtain globally optimized parameters. The titration data obtained using the ^{1}H NMR titration method were analyzed by fitting to a simple 1:1 binding isotherm using a nonlinear curve fitting program developed by one of us (C.A.H.).

Synthesis. Compounds **5a**,[6] **5b**,[7] **6**,[8] and **7**[9] were prepared as described previously. Compound **8** was prepared by coupling reaction of the corresponding commercially available acid chloride with diethylamine.

***N,N′*-Bis(3,5-dimethyl-4-pyridinyl)-4-ethoxy-2,6-pyridinedicarboxamide (3a).** To a CH_2Cl_2 (10 mL) solution of 4-ethoxy-2,6-pyridinedicarbonyl dichloride (**5a**) (660 mg, 2.3 mmol) cooled at 0 °C were added a solution of 4-amino-3,5-lutidine (**6**) (607 mg, 5 mmol) in CH_2Cl_2 (10 mL) and *N,N*-diisopropylethylamine (1 mL, 5.8 mmol). The solution was stirred under argon atmosphere at room temperature for 2 h and was subsequently heated at reflux for 2 h. The reaction mixture was diluted with CH_2Cl_2 (10 mL), washed twice with saturated $NaHCO_3$ solution and once with brine, dried over anhydrous $MgSO_4$, filtered, and evaporated in vacuo. The solid residue was washed with diethyl ether and was recrystallized in CH_2Cl_2/EtOAc solvent to yield **3a** as a white solid (190 mg, 56%): mp 238−240 °C; IR (KBr, cm^{-1}) 3294, 1669, 1587, 1506, 1342, 1166, 1044, 685; ^{1}H NMR (300 MHz, $CDCl_3$) δ 9.60 (s, NH, 2H), 8.30 (s, 4H), 7.97 (s, 2H), 4.31 (q, J = 6.9 Hz, 2H), 2.25 (s, 12H), 1.50 (t, J = 6.9 Hz, 3H); ^{13}C NMR (75 MHz, $CDCl_3$) δ168.7, 161.5, 150.6, 149.7, 142.1, 130.3, 112.7, 64.5, 15.9, 14.7; HRMS *m/z* (ESI) calcd for $C_{23}H_{25}N_5O_3$ [M + H$^+$] 420.2036; found, 420.2047; calcd for $C_{23}H_{25}N_5O_3Na$ [M + Na$^+$] 442.1853; found, 442.1866.

***N,N′*-Bis(3,5-dimethyl-4-pyridinyl)-5-methoxy-1,3-benzenedicarboxamide (3b).** To a CH_2Cl_2 (6 mL) solution of 4-methoxy-1,3-benzenedicarbonyl dichloride (**5b**) (187 mg, 0.8 mmol) cooled at 0 °C were added 4-amino-3,5-lutidine (**6**) (206 mg, 1.7 mmol) and *N,N*-diisopropylethylamine (365 μL, 2.1 mmol). The reaction mixture was stirred under argon atmosphere for 2 h at room temperature followed by heating at reflux for an additional 2 h. The reaction mixture was filtered, and the filtrate was washed twice with saturated $NaHCO_3$ solution and once with brine, dried over anhydrous Na_2SO_4, filtered, and evaporated in vacuo. The solid residue was triturated with diethyl ether affording **3b** as a white solid (70 mg, 22%). mp 229−234 °C; IR (KBr, cm^{-1}) 3415, 3232, 1653, 1592, 1514, 1383, 1344, 1162, 1055, 879, 700; ^{1}H NMR (300 MHz, $CDCl_3$) δ 8.36 (s, 4H), 8.09 (s, 1H), 7.91 (s, 2H), 7.67 (s, 2H), 3.95 (s, 3H), 2.25 (s, 12H); ^{13}C NMR (75 MHz, $CDCl_3$) δ 164.19, 160.49, 149.55, 141.70, 135.62, 129.68, 117.98, 116.86, 50.04, 15.47; HRMS *m/z* (ESI) calcd for $C_{23}H_{25}N_4O_3$ [M+H$^+$] 405.1927; found, 405.1939.

Free Base Bisporphyrin ($4aH_2$). A solution of aminoporphyrin **7** (100 mg, 0.12 mmol), freshly distilled dry triethylamine (40 μL, 0.28 mmol), and a catalytic amount of 4-(dimethylamino)pyridine (DMAP) in dry CH_2Cl_2 (10 mL) was cooled at 0 °C in an ice−water bath, and diacid chloride **5a** (13 mg, 0.05 mmol) dissolved in a minimum amount of dry CH_2Cl_2 was added in one portion. After stirring for 3 h at room temperature under argon atmosphere, the mixture was heated at reflux for 2 h and was cooled again at room temperature. The organic layer was washed with 0.1 N HCl, saturated $NaHCO_3$, and brine; dried over Na_2SO_4; filtered; and concentrated in vacuo to yield a solid residue. The product was separated from the unreacted porphyrin by flash chromatography of the solid residue on silica gel eluting with CH_2Cl_2:hexanes (2:1) to recover first the unreacted aminoporphyrin **7** and affording next the free base bisporphyrin **$4aH_2$** as a purple solid (50 mg, 46%): ^{1}H NMR (300 MHz, $CDCl_3$) δ 10.04 (s, 2H), 8.89 (m, 16H), 8.33 (d, J = 8.5 Hz, 4H), 8.25 (d, J = 8.5 Hz, 4H), 8.19 (s, 2H), 8.10 (d, J = 7.9 Hz, 12H), 7.54 (m, 12H), 4.43 (q, J = 6.7 Hz, 2H), 2.94 (m, 12H), 1.89 (m, 12H), 1.62 (t, J = 6.7 Hz, 3H), 1.51 (m, 24H), 1.02 (m, 18H), −2.77 (s, 4H).

Free Base Bisporphyrin ($4bH_2$). Aminoporphyrin **7** (220 mg, 0.26 mmol), freshly distilled dry triethylamine (60 μL, 0.4 mmol), and a catalytic amount of 4-(dimethylamino)pyridine (DMAP) were dissolved in dry CH_2Cl_2 (30 mL), and the resulting solution was cooled at 0 °C in an ice−water bath. Diacid chloride **5b** (31 mg, 0.13 mmol) was added in one portion to the previously cooled reaction mixture. After stirring for 4 h at room temperature under argon atmosphere, the organic layer was washed with saturated $NaHCO_3$ and brine, dried over Na_2SO_4, filtered, and concentrated in vacuo to yield a solid residue. The product was separated from the unreacted porphyrin by flash chromatography of the residue on silica gel eluting with CH_2Cl_2:THF (99:1) to recover first the aminoporphyrin **7** (39 mg) and affording next the free base bisporphyrin **$4bH_2$** as a purple solid (100 mg, 42%):^{1}H NMR (300 MHz, $CDCl_3$): δ 8.89 (s, 8H), 8.87 (s, 8H) 8.35 (s, 2H), 8.29 (d, 4H, J = 8.2 Hz), 8.26 (s, 2H), 8.12 (d, 4H, J = 8.2 Hz), 8.11 (d, 12H, J = 7.8 Hz), 7.84 (s, 2H), 7.55 (d, 12H, J = 7.8 Hz), 2.94 (t, 12H, J = 7.5 Hz), 1.90 (m, 12H), 1.52 (m, 24H), 1.02 (t, 18H, J = 7 Hz), −2.75 (s, 4H).

General Procedure for the Preparation of the Zinc Bisporphyrins 4a−b. The free base bisporphyrin (100 mg, 0.05 mmol) was dissolved in CH_2Cl_2−CH_3OH (3:1, 30 mL), and zinc acetate (180 mg, 0.98 mmol) was added. The reaction mixture was protected from light and was stirred at room temperature for 1 h. After removal of the solvents under reduced pressure, the product was purified by column chromatography on basic alumina eluting with CH_2Cl_2:CH_3OH (99:1). The product was recrystallized from CH_2Cl_2:CH_3OH yielding the zinc bisporphyrin **4**.

Zn Bisporphyrin (4a). (87 mg, 82%); mp > 220 °C dec; IR (KBr, cm^{-1}) 3414, 2924,1618, 1525, 1384, 1338, 1205, 998, 796, 719, 621;^{1}H NMR (300 MHz, $CDCl_3$) δ 10.03 (s, 2H), 8.99 (m, 16H), 8.32 (d, 4H, J = 8.8 Hz), 8.24 (d, 4H, J = 8.8 Hz), 8.16 (s, 2H), 8.10 (d, 12H, J = 8.0 Hz), 7.53 (dd, 12H, J = 8.0, 2.5 Hz), 4.42 (q, 2H, J = 6.9 Hz), 2.94 (m, 12H), 1.91 (m, 12H), 1.62 (t, 3H, J = 6.9 Hz), 1.52 (m, 24H), 1.02 (m, 18H); HRMS *m/z* (ESI) calcd for $C_{127}H_{123}N_{11}O_3Zn_2$ 1977.8393; found, 1977.8372.

Zn Bisporphyrin (4b). (96 mg, 94%); mp 295−300 °C; IR (KBr, cm^{-1}) 3415, 2926, 1617, 1526, 1384, 1339, 1207, 1000, 797, 720; ^{1}H NMR (300 MHz, $CDCl_3$) δ 8.99 (s, 8H), 8.98 (d, 4H, J = 5.3 Hz), 8.96 (d, 4H, J = 5.3 Hz), 8.26 (d, 4H, J = 8.5 Hz), 8.19 (s, 2H), 8.12 (d, 4H, J = 8.2 Hz), 8.11 (d, 8H, J = 8.2 Hz), 7.94 (d, 4H, J = 8.5 Hz), 7.82 (s, 1H), 7.57 (s, 2H), 7.56 (d, 4H, J = 8.2 Hz), 7.53 (d, 8H, J = 8.2 Hz), 3.96 (s, 3H), 2.95

(m, 12H), 1.92 (m, 12H), 1.50 (m, 24H), 1,02 (m, 18H); HRMS *m/z* (ESI) calcd for $C_{127}H_{122}N_{10}O_3Zn_2Na$ 1989.8187; found, 1989.8251.

***N,N′*-Dioctyl-hexanediamide (9).** A suspension of adipic acid (0.3 g, 2 mmol) in thionyl chloride (4 mL) containing a catalytic amount of triphenyl phosphine was heated at reflux until a clear solution was obtained (~2 h). The excess of thionyl chloride was removed and the residue was suspended in dry CH_2Cl_2 (10 mL). To this solution, octylamine (680 μL, 4.1 mmol) and triethylamine (600 μL, 4.3 mmol) were added. The reaction mixture was stirred overnight; washed with aqueous HCl (5%), NaOH solution (10%), and brine; dried over Na_2SO_4; filtered; and concentrated. The residue was purified by column chromatography (CH_2Cl_2/MeOH 5%) to give **9** as a white solid (320 mg, 43%): IR (KBr, cm^{-1}) 3313, 1632; ^1H NMR (300 MHz, $CDCl_3$) δ: 5.62 (s, 2H), 3.24 (m, 4H), 2.19 (m, 4H), 1.65 (m, 4H), 1.49 (t, 4H, J = 5.8 Hz), 1.27 (m, 20H), 0.88 (m, 6H). Anal. Calcd (%) for $C_{22}H_{44}N_2O_2$ (368.59): C 71.69, H 12.03, N 7.60. Found: C 71.42, H 12.20, N 7.62.

2D-EXSY Experiment. The 2D-EXSY experiment was recorded at 253 K on a 300 MHz spectrometer using an inverse probe. The mixing time was 200 ms. Exchange cross-peaks were integrated using XWINNMR Bruker software. The calculated integrations were processed using the program D2DNMR[21] considering a three-site exchange to give the chemical exchange rate constants $k_{macrocycle}$ and $k_{rotaxane}$.

Acknowledgment. We thank Dirección General de Investigación, Ministerio de Ciencia y Tecnología (BQU2002-04651) for grant support. P.B. and A.I.O. also thank ICIQ Foundation for financial support. A. F. thanks MCyT for a Ramón y Cajal contract. Thanks are also due to Professor Kyu-Sung Jeong for providing us with a sample of compound **10**.

Supporting Information Available: UV−vis and ^1H NMR spectra recorded during titrations of **4a** with **3a**. Aromatic region of the ^1H NMR spectra recorded during titration of **1aa** with **8**. Selected expansions of the ROESY experiments performed on (1) the self-assembled macrocycle **1aa** and on (2) the pseudorataxane complex **1aa·8**. ^1H NMR spectra of compounds **3a** and **4a**. This material is available free of charge via the Internet at http://pubs.acs.org.

JO0505369